High Energy Physics and Nuclear Physics

Volume 21, Number 4

Correlation Between Sun Shadows of 10 TeV Cosmic Ray and the Solar Activity

Liu Shaomin[1], Ding Linkai[1], Shi Ce[1], Zhaxiciren[2], Zhaxisanzhu[2],
Mu Jun[4], Wnag Hui[1], Lu Hong[1], Feng Zhenyong[3], Ren Jingru[1], Yu Guangce[3],
Zhou Wende[4], Labaciren[2], Meng Xianru[2], Meng Lie[1], Zhang Jilong[1],
Zhang Chunsheng[1], Zhang Huimin[1], Shi Zhizheng[1], Jia Huanyiu[3],
Mei Dongming[2], Huang Qing[3],Tan Youheng[1], Huo Anxiang[1], and Dai Benzhong[4]

[1](Institute of High Energy Physics, Chinese Academy of Sciences, Beijing, China)
[2](Cosmic Ray Institute, Tibet University, Lhasa, China)
[3](Department of Physics, South West Jiaotong University, Chengdu, China)
[4](Department of Physics, Yunnan University, Kunming, China)

Using data obtained in the period of June 1990–October 1993, the shadows of the Sun and the Moon have been detected at 5.7 σ and 7.1 σ levels, respectively, in the 10TeV cosmic ray flux by the Tibet air shower array at an altitude of 4300 m above sea level. The shadow of the Sun is found to be deflected away from the Sun by 0.62° to the west and 0.22° to the south by the interplanetary magnetic field. The correlation between the shadow of the Sun and the solar activity and its asymmetry are studied in detail. A new qualitative explanation to the shift and yearly variation of the Sun's shadow is presented.

Key words: cosmic rays, interplanetary magnetic field (IMF), solar activity.

1. INTRODUCTION

Charged primary cosmic rays will be bent by the interplanetary magnetic field (IMF) while they propagate through interplanetary space before arrive they at Earth. Since 1957 Clark [1] indicated that

Received on January 13, 1997. Supported by the National Natural Science Foundation of China and the Chinese Academy of Sciences.

the Sun and the Moon could make shadows in the high energy cosmic ray flux, and the measurement of the shadows could refer to new knowledge of the magnetic fields of these celestial objects, and so many kinds observations have been proposed. However, all of them were not put into effect limited by the experimental technique. In recent years, several groups including the Sino-Japan cooperative Yanbajing Experiment Group have started to observe the shadows of the Sun and the Moon as the standard check of the pointing resolution of air shower arrays. Because only the Yangbajing array could work in a lower energy (10 TeV) region, it uniquely observed the deflection of cosmic ray shadows by the Sun, the first time observed the effect of IMF on 10 TeV cosmic rays [2]. In addition, Yangbajing data indicated the yearly variation of the Sun's shadow and the different shifts in the Away sector and the Toward sector of the IMF [3, 4]. Using data obtained by the Tibet air shower array, the correlations between 10 TeV cosmic ray shadow of the Sun and the solar activity and its asymmetry are studied in this paper. A new qualitative explanation to the shift and yearly variation of the Sun's shadow is presented.

2. EXPERIMENTAL ARRANGEMENT

2.1. Experiment facility

The Tibet extensive air shower (EAS) array is located at Yangbajing in Tibet (90.53 °E, 30.11 °N, altitude 4300 m a.s.l., air depth 606 g/cm^2). The first phase array has been running from June 1990 until October 1993 that consists of 45 fast timing (FT) scintillation detectors of 0.5 cm^2 each, which are placed in a 7 × 7 grid pattern of 15 m spacing. The FT array is surrounded by 16 density detectors in order to achieve a good core location for each shower event. A lead plate of 5 mm thickness is placed on the top of each detector to improve the pointing resolution by converting some gamma rays in air showers to elector pairs. The detector arrangement is schematically shown in Fig. 1. The main physics goal of Tibet EAS array is to search for gamma ray point sources in the 10 TeV region.

A CAMAC bus is used in the on-line data acquisition system which is controlled by a 32-bit micro-computer. Signals received from FT detectors are used to generate triggers. The analog/digital converter (ADC) and time/digital converter (TDC) channels of the array's electronics measure the number of shower particles hit into each detector and their relative arrival time, respectively. A rubidium clock records the real arrival time of each shower. The primary energy of each shower can be gauged by the ADC counts of all channels, and its arrival direction can be reconstructed by the TDC counts of each channel. The celestial coordinates for each event can be calculated from its arrival

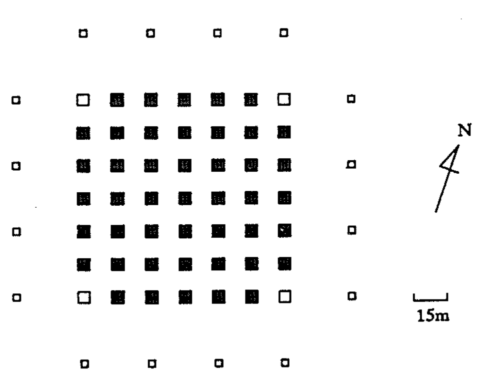

Fig. 1

Schematic view of the Tibet EAS array. Solid squares stand for the FT detectors. Open squares stand for density detectors.

time and direction. So, the Sun's shadow of cosmic rays can be plotted by the database of a large amount of shower events. The raw data is recorded in an 8-mm tape of 2.3 Gbyte capacity by EXB-8200 tape driver. For the stable running of the whole detector system, a multiple calibration is employed. At the beginning of each run, a TDC test module is used to calibrate TDCs. The laser calibration system [5] is adopted to monitor the relative offset-time, gain, and linearity of photomultiplier tubes (PMT) at regular time intervals.

During the period from June 1990 to September 1992, the first phase array is triggered at a rate of 20 Hz by any four-fold coincidence of FT detectors. From September 1992 to October 1993, the trigger condition is changed as any three-fold coincidence which results in a rigger rate of 40 Hz.

2.2. Event selection criteria

The EAS event selection criteria are as following:

(1) Each of the four- (or three-)fold FT detectors should detect a signal which corresponds to more than 1.25 particles.

(2) Among the fired detectors which record the highest particle densities, two or more should be in the inner 5 $\times$ 5 detectors.

According to the results of Monte Carlo simulation of the array's performance, the mean energy is about 10 TeV for all events satisfying the conditions (1) and (2). Among all events, the mean energy of those for more than 100 particles are detected by FT detectors is 35 TeV.

Among 4.5 $\times$ 10^8 events thus selected, there are 2.77 $\times$ 10^6 and 2.07 $\times$ 10^6 events arriving around 8° from the Sun and the Moon, respectively, and with a zenith angle less than 50°. These events are used to analyze the Sun and Moon shadows.

During the data analysis a coordinate system was fixed on the object, putting the origin of coordinates at its center (the Sun or the Moon). The position of each event in this coordinate system is specified by the angular distance θ and position angle ϕ between the arrival vector of the event and

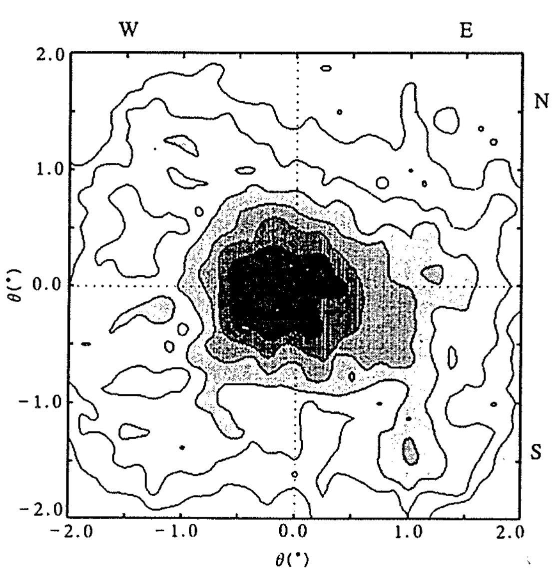

Fig. 2

Contour map of the weights of deficit event density around the Moon in the area of 4° $\times$ 4° centered at the Moon. The contour lines are drawn from a level of no deficit, 0 σ, with a step of 1 σ.

the position vector of the Sun and Moon. The equatorial coordinate is used for the Moon and the ecliptic coordinate for the Sun, respectively. The shadows of the Sun or the Moon can be studied by the distribution of the weight of the deficit event density (which is defined as $(N_{src} - N_{bg})/\sqrt{N_{bg}}$, where N_{src} and N_{bg} are the on-source and off-source event densities, respectively) around the Sun or Moon.

3. MOON SHADOW AND ARRAY PERFORMANCE

The array performance such as the angular resolution can be examined by observing the Moon's shadow that in our analysis is shown in Fig. 2 for all events. The Moon's shadow is seen to be shifted westward slightly. Using the maximum likelihood method [2, 7, 8], the angular resolution of the array is found to be $0.85^{+0.09}_{-0.07}(°)$ with a significance of 7.1 σ. The maximum deficit position of the shadow profile is found at 0.11° ± 0.07(°) to the west and 0.02 ± 0.07(°) to the south. The deflection of the incident positively charged particles in the space between the Moon and Earth is mainly induced by the geomagnetic field. So, the Moon's shadow reflects the modulation effect of geomagnetic field on primary cosmic ray particles. Under a dipole field approximation, the Monte Carlo simulation [2] indicated that the Moon's shadow will be bent to the west by about 0.15° for all selected events corresponding to the mean energy of 10 TeV. Our result is consistent with this prediction within the error. Because cosmic rays under the deflection of the geomagnetic field will make the position of the Moon's shadow only shift in the east-west direction, the deflection in the north-south direction of the Moon's shadow could be regarded as the systematic pointing error of the array. From Fig. 2, it can be found that the Moon's shadow is shifted a little in the north-south direction showing that the systematic pointing error of Tibet EAS array is less than 0.1°. The result of the Moon's shadow is not only regarded as the test of array performance and the data quality and reliability, but also regarded as the standard reference of the Sun's shadow.

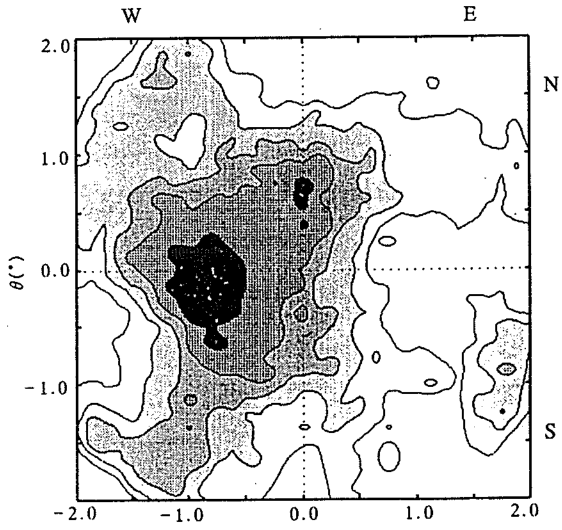

Fig. 3

Contour map of the weights of deficit event density around the Sun in the area of 4° × 4° centered at the Sun. The contour lines are drawn from a level of no deficit, 0 σ, with a step of 1 σ.

4. SUN SHADOW

The Sun's shadow for all events with the mean energy of 10 TeV in our analysis is shown in Fig. 3. Assuming a Gaussian distribution for the event deficit density around the Sun, the maximum likelihood analysis shows that the most probable position of the center of the deficit is at $0.62 \pm 0.12(°)$ to the west and $0.22 \pm 0.18(°)$ to the south when the 1.06° angular resolution of the array is used. The logarithm likelihood is calculated to be 16.7 at this position with a significance of $5.7\ \sigma$. Compared with the Moon's shadow, when the geomagnetic field effect is ignored, the position of the Sun's shadow is seen to be remarkably shifted from the center of the Sun. With the increasing energy, the deflection of cosmic ray particles by the IMF is expected to be weaker and the position of the Sun's shadow will approach the apparent center of the Sun. When the event sample with the mean energy of 35 TeV is chosen, the position of the Sun's shadow is shown to be located at $0.22 \pm 0.18(°)$ to the west and $0.16 \pm 0.18(°)$ to the south. Due to a fewer number of events, the significance decreases to $5.5\ \sigma$.

In order to study the effect of the IMF on the deflection of the position of the Sun's shadow, the Sun's shadows of 10 TeV cosmic rays are studied separately when the Earth is in the Away sector and the Toward sector of the IMF. For sectors in which the magnetic field is directed away from the Sun, the center position of the Sun's shadow is obtained at 0.83° to the west and 0.28° to the north; whereas for the Toward sectors, it is at 0.56° to the west and 0.45° to the north. It can be known that from the magnetic structure of IMF, the azimuthal components of the Archimedean spiral magnetic field in the Away sectors and Toward sectors will make the Sun's shadows shift to the north or south, respectively. Our observation results confirmed that the IMF has the main effect on the deflection of the position of the Sun's shadow which is consistent with the expectation.

In order to observe the important influence of the solar activity upon the IMF, the monthly shadow of the Sun is studied using the data in the period of June to October 1990 when the Sun was near its maximum phase. Although the number of events is too few to make an excellent statistical calculation the result still shows during this period an apparent variation trend of the Sun's shadow. The monthly change of the positions of the Sun's shadow is shown in Table 1.

The analysis of the Sun's shadow in the boundary of IMF shows that in the period when the magnetic field changed its direction from Away to Toward or from Toward to Away the Sun's shadow is almost consistent with those in Toward or Away sectors, respectively. It should be noted that here the mean time delay of 4.5 days is taken into account from the speed of the solar wind propagation from the Sun to the Earth.

The yearly variations of the positions of the Sun's shadow and in both Away and Toward sectors in 1990 to 1993 are studied also. The results are summarized in Table 2 from which it can be seen that there exists the yearly decrease of the deflection of the positions of Sun shadows with the change of the solar activity, which is consistent with that reported in Ref. [4].

5. DISCUSSION AND CONCLUSION

The IMF is shown to have the main effect on the deflection of the Sun's shadow. The azimuthal component of the IMF in the Toward sector makes the positively charged cosmic ray particles bend to the north when they propagate through the interplanetary space. So, the Sun's shadow in the Toward sector shifts to the south. Similarly, the IMF in the Away sector makes the shadow shift to the north. According to the solar geophysical data (SGD, NOAA/USAF), in the period from 1990 to the middle of 1991, the Sun was in its maximum phase, then turned to the declining phase gradually. At that time, the solar magnetic field had large deviations from a pure dipole, i.e., a small contribution was from a dipole with large contributions from higher multi-poles, and the dipole field axis was almost sideways, especially in the period from 1990 to 1991 just after the reversal of the solar polar fields. Around the middle of 1991, the largest inclination (67°) of the neutral sheet to the ecliptic plane was

Table 1

Positions of the Sun's shadow in the maximum phase of solar activity.

Year	Position	Significance
July 1990	0.6°W, 1.2°S	1.4 σ
August 1990	1.0°W, 0.5°S	1.5 σ
September 1990	1.5°W, 0.6°N	1.5 σ

Table 2

The yearly variation of the positions of the Sun's shadow.

Year	Position of the sun's shadow (°)	Position (away) (°)	Position (toward) (°)
1990	0.8W, 0.1S 2.3 σ	1.0W, 0.2N 2.1 σ	0.4W, 0.3S 1.9 σ
1991	0.7W, 0.8S 3.7 σ	0.9W, 0.3N 2.7 σ	0.6W, 0.9S 3.4 σ
1992	0.3W, 0.5N 3.9 σ	0.2W, 0.5N 3.1 σ	0.4W, 0.0S 2.9 σ
1993	0.2W, 0.0S 2.6 σ	0.3W, 0.1N 2.1 σ	0.5W, 0.2S 2.3 σ
1990–1993	0.6W, 0.2S 5.7 σ	0.8W, 0.3N 4.5 σ	0.5W, 0.4S 4.9 σ

observed. Meanwhile, large solar flares were sometimes observed during that period. The analysis of the yearly variations of the Sun's shadow shows that there possibly exist yearly large-scale changes of the solar and interplanetary magnetic fields which result in the strong modulation of the solar activity on the positions of the Sun's shadow. The different movement of the Sun's shadow in the Toward sectors and Away sectors may be caused by the effect of varying waviness of the current sheet of the large-scale magnetic fields.

The solar activity is known to be asymmetric on the northern and southern hemispheres in a solar cycle. As a long-term result of this kind of a symmetry, the mean position of the neutral sheet of IMF is displaced away from the ecliptic plane to the north or south [9, 10]. In the period of 1990 to 1993, sunspots, which are the indication of the solar activity, dominated on the Southern Hemisphere which resulted in the mean position of the neutral sheet being displaced to the north of the ecliptic plane. Thus the IMF polarity above the neutral sheet directed away from the Sun, and toward the Sun below the neutral sheet. So, the number of days when IMF was directed toward the Sun observed in the Earth is larger than that when IMF directed away from the Sun. During the period of 1990 to 1993, the effective observation days of Toward and Away sectors were 593 and 537, respectively, i.e., the Away sector dominated in IMF slightly. Therefore, the Sun's shadow was shifted to the South overall during 1990 to 1993. The distribution of the Toward sector in the southern part of the neutral sheet and the Away sector to the north of the neutral sheet forms the magnetic field component which makes the Sun's shadow shift to the west. For the Sun's shadows in the Toward and Away sectors, all shift to the west.

The change of the mean position of the neutral sheet revealed by the number of days when the IMF directed Toward and Away is the result of the sunspots' asymmetry on both hemispheres of the Sun. From this point of view, the yearly change of the Sun's shadow could be explained qualitatively. In the 4 years from 1990 to 1993, the effective observation days of the Toward and Away sectors are 79_T and 65_A for 1990, 143_T and 139_A for 1991, 142_T and 148_A for 1992, 132_T and 116_A for 1993, respectively. Combined with the number of relative sunspots, it can be found that during this period, the Toward sector dominated for 3 years except in 1992, while in 1992 the Away sector of IMF dominated slightly. This is consistent with the observation of the yearly variation of the Sun's shadows listed in Table 2. In summary, the analysis of the yearly variation of the Sun's shadows in 10 TeV cosmic ray flux shows that there exists a direct correlation between the Sun's shadows and its yearly variation of the solar activity and its asymmetry on both hemispheres.

As the asymmetry of solar activity is concerned, the position of the Sun's shadow over a long time is expected to change in both north-south and west-east directions in a solar cycle. This change should be further confirmed by continuous observations in the minimum phase, the increasing phase, and nearly the maximum phase of solar activity by the Tibet EAS array. The effective area of the second phase of the Tibet EAS array is increased by a factor of about 8. The new phase array has been running since October 1995. At present, the Sun is in its minimum phase, and will reach its maximum at around 2000. We hope the continuous observation of the second phase array will provide further understanding of the correlation between Sun's shadows and the solar activity, so as to provide a new overall monitor for the solar magnetic field, IMF, and its variability.

ACKNOWLEDGMENTS

The authors would like to express their gratitude to all the members of Japanese collaborators led by Prof. Yuda, Institute for Cosmic Ray Research (ICRR), Tokyo University. It was the common effort of Chinese and Japanese researchers that lead to the successful observation of the Tibet EAS array.

REFERENCES

[1] G.W. Clark, *Phys. Rev.*, **108**(1957), p. 450.
[2] M. Amenomori *et al.*, *Phys. Rev.*, **D47**(1993), p. 2675.
[3] M. Amenomori *et al.*, *ApJ*, **415**(1994), L147.
[4] M. Amenomori *et al.*, *ApJ*, **464**(1996), p. 954.
[5] M. Nishizawa *et al.*, *Nucl. Instrum. Methods*, **A285**(1989), p. 532.
[6] M. Amenomori *et al.*, *High Energy Phys. Nucl. Phys.* (Chinese Edition), **17**(1993), p. 385.
[7] D.E. Alexandreas *et al.*, *Phys. Rev.*, **D43**(1991), p. 1735.
[8] Li Tipei, *Mechanics Processure of Experiment*, Science Press, China, 1980.
[9] D.B. Swinson, *Proc. 21th ICRC, Adelaide, Australia*, SH.6.2-2, 1991.
[10] D.B. Swinson, *Proc. 21th ICRC, Adelaide, Australia*, SH.6.2-3, 1991.